Article details

Sarris A.J.C., Hansen T., Geus M.A.R. de, Maurits E., Doelman W., Overkleeft H.S., Codée J.D.C., Filippov D.V. & Kasteren S.I. van (2018), Fast and pH-Independent Elimination of trans-Cyclooctene by Using Aminoethyl-Functionalized Tetrazines, Chemistry-a European Journal 24(68): 18075-18081.
Doi: 10.1002/chem.201803839

ChemPubSoc Europe

DOI: 10.1002/chem.201803839

CHEMISTRY A European Journal Full Paper

Bioorthogonal Chemistry

Fast and pH-Independent Elimination of *trans*-Cyclooctene by Using Aminoethyl-Functionalized Tetrazines

Alexi J. C. Sarris, Thomas Hansen, Mark A. R. de Geus, Elmer Maurits, Ward Doelman, Herman S. Overkleeft, Jeroen D. C. Codée, Dmitri V. Filippov,* and Sander I. van Kasteren*[a]

Abstract: The inverse-electron-demand Diels–Alder/pyridazine elimination tandem reaction, in which the allylic substituent on *trans*-cyclooctene is eliminated following reaction with tetrazines, is gaining interest as a versatile bioorthogonal process. One potential shortcoming of such currently used reactions is their propensity to proceed faster and more efficiently at lower pH, a feature caused by the nature of the tetrazines used. Here, we present aminoethyl-substituted tetrazines as the first pH-independent reagents showing invariably fast elimination kinetics at all biologically relevant pH values.

Introduction

Bioorthogonal chemistry, the execution of selective chemical conversions within a biological sample, has provided a wealth of information on a wide variety of biological processes.[1] Initial work focused on controlled ligation reactions within biological systems through the use of copper-catalyzed Huisgen cycloaddition,[2] Staudinger ligation,[3] inverse-electron-demand Diels–Alder (IEDDA),[4] and other chemistries[5] to introduce reporter groups while minimally impacting the biological processes being studied.

Recently, bioorthogonal reactions have also been used to unmask functional groups in living systems.[6] The IEDDA/pyridazine elimination reaction,[7] a "click-to-release" reaction in which an allylic substituent on *trans*-cyclooctene (2-TCO, axial (*E*)-cyclooct-2-en-1-ol) is eliminated upon rearrangement of the pyridazine intermediate, has proven particularly favorable in this regard and it shows excellent biocompatibility[8] and low toxicity.[9] In vivo applications include the chemical control of drug release,[10] control over T-cell activation,[11] release of drugs from hydrogels,[12] as well as control over kinase activity in mice.[9]

Mechanistic insights into this reaction have provided a pathway to improving this ligation/elimination reaction.[13] Chen and co-workers, for example, discovered that asymmetric tetrazines carrying both an electron-donating and -withdrawing substituent showed a significant improvement in the elimination rates compared with their symmetric counterparts, leading to improved results with their most prominent tetrazine **1** compared with 3,6-dimethyltetrazine (**2**; Figure 1).[13a] Weissleder and co-workers used carboxy-functionalized tetrazine **3** (Figure 1), which also resulted in elimination rates much faster than with tetrazine **2**.[13b] It was also discovered that, for tetrazines containing simple alkyl substituents, the elimination rates are very sensitive to the pH of the reaction medium: Although release is completed within an hour under acidic conditions (tetrazine **2**, pH 5.0), it takes several hours under physiological conditions (tetrazine **2**, pH 7.0),[13b] as the elimination step is subject to general acid catalysis.

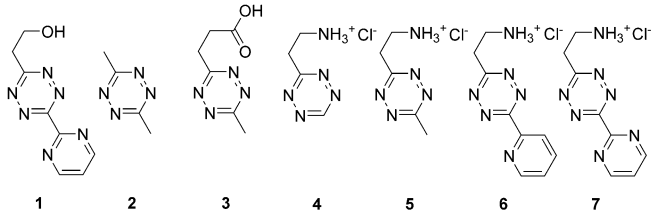

Figure 1. Known tetrazines (**1**–**3**) and aminoethyltetrazines designed in this study (**4**–**7**).

What is currently lacking are tetrazines that maintain fast elimination kinetics over the whole biologically relevant pH range (pH 3.5–7.5). We postulated that tetrazines **4**–**7** (Figure 1) could serve as pH-independent eliminating tetrazines. The amine on the aminoethyl substituent, as a cationic ammonium functionality at and below physiological pH, would function as a general acid during the elimination step, thereby potentially improving both the release rate and efficiency.

[a] *A. J. C. Sarris, T. Hansen, M. A. R. de Geus, E. Maurits, W. Doelman, Prof. H. S. Overkleeft, Dr. J. D. C. Codée, Dr. D. V. Filippov, Dr. S. I. van Kasteren*
Leiden Institute of Chemistry
and The Institute for Chemical Immunology, Leiden University
Einsteinweg 55, 2333 CC Leiden (The Netherlands)
E-mail: filippov@lic.leidenuniv.nl
s.i.van.kasteren@chem.leidenuniv.nl

Supporting information and the ORCID identification number(s) for the author(s) of this article can be found under: https://doi.org/10.1002/chem.201803839. It contains full experimental details.

Here we describe the design, synthesis, and characterization of a new family of tetrazines based on this premise. We show that, through intramolecular proton delivery, an 18-fold increase in the elimination rate compared with the fastest rates reported in the literature, with tetrazines **1** and **3**, could be attained. Furthermore, this intramolecular proton source renders the reaction pH-independent with minimal change in the reaction rates from pH 3 to pH 7.4.

Results and Discussion

Design

We hypothesized that the presence of an aminoethyl functionality could serve as intramolecular catalyst for both the 4,5- to 1,4-dihydro tautomerization and subsequent elimination process (Scheme 1). Tetrazines can add to 2-TCO in two ways with

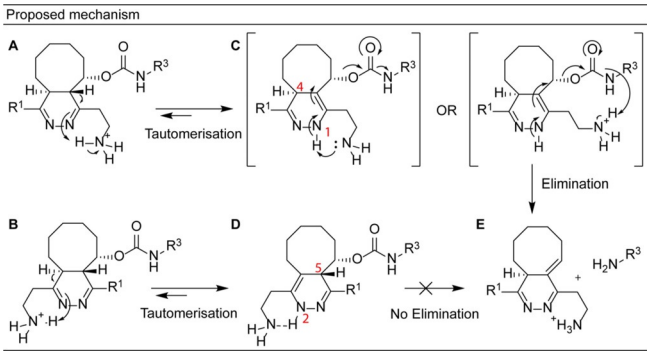

Scheme 1. Proposed mechanism for the tautomerization and elimination by intramolecular catalysis by the aminoethyl functionality.

the aminoethyl functionality positioned at either the eliminating end (**A**, "head-to-head" adduct) or the non-eliminating end (**B**, "head-to-tail" adduct). In the "head-to-head" adduct **A**, the tautomerization of the initial 4,5-tautomer may be promoted leading to either the eliminating (**C**) 1,4-tautomer or non-eliminating (not shown) 2,5-tautomer. The same applies to **B**, in which the tautomerization leads to either the eliminating 1,4-tautomer (not shown) or non-eliminating (**D**) 2,5-tautomer. Elimination (**E**) may then be driven through the proximity of the intramolecular catalytic site to both the N-1 atom of the dihydropyridazine core and the carbamate linkage.

To investigate the behavior of tetrazines **4**–**7**, DFT calculations were performed (see Figures S1–S4 in the Supporting Information).[14] The transition state of the cycloaddition step was evaluated computationally by using the reported transition states as initial guesses.[14] All the structures were optimized with Gaussian 09[15] by using the ωB97XD long-range-corrected hybrid functional and 6-31+G(d) as basis set. Optimization was performed in combination with a polarizable continuum model (PCM) using water as the solvent.

In the initial IEDDA reaction, the "head-to-head" adduct was favored over the "head-to-tail" adduct for all the studied tetrazines (Figure 2). For example, the "head-to-head" transition state (**TS-1**, Figure 2A) for tetrazine **5** proved to be 3.5 kcal mol^{-1} lower than the "head-to-tail" transition state (**TS-2**, Figure 2B). The thermodynamic preferences for the other aminoethyltetrazines **4**, **6**, and **7** appear to be even greater at 4.4–4.6 kcal mol^{-1} (Figure 2C). For the "head-to-head" transition states, the cationic ammonium functionality shows an interaction with the carbamate linkage resulting in an energetically more favorable approach.

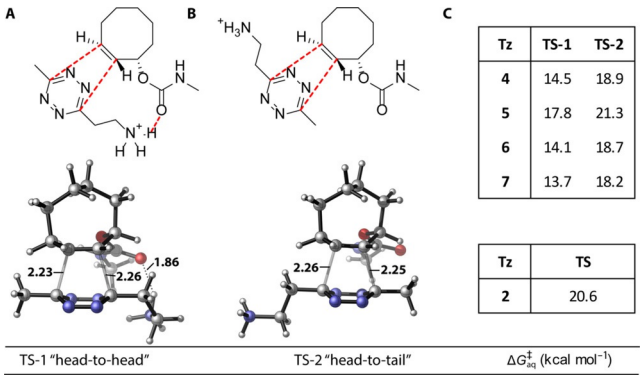

Tz	TS-1	TS-2
4	14.5	18.9
5	17.8	21.3
6	14.1	18.7
7	13.7	18.2

Tz	TS
2	20.6

Figure 2. ωB97XD/6-31+G(d)-optimized transition states for the head-to-head (**TS-1**) and head-to-tail (**TS-2**) reactions of tetrazines with the model axial (*E*)-cyclooct-2-ene. A) Head-to-head transition state with 3-aminoethyl-6-methyltetrazine (**5**). B) Head-to-tail transition state with 3-aminoethyl-6-methyltetrazine (**5**). C) Transition-state energies of **TS-1** and **TS-2** for tetrazines **2** and **4**–**7**. $\Delta G^{\ddagger}_{aq}$ values shown in kcal mol^{-1}.

After establishing the theoretically favored geometries of the transition states in the IEDDA step, which lead to the "head-to-head" adduct, we investigated the lowest-energy geometries of the formed adducts with respect to the feasibility of intramolecular proton transfer from the ammonium functionality. Towards this end we generated a conformer distribution, with the Spartan 10 program[16] using molecular mechanics with MMFF94 as force field, for the initially formed 4,5-tautomer and subsequent 1,4-tautomer after cycloaddition of a model TCO to tetrazines **2** and **5**. All the generated structures were further optimized in the gas phase with Gaussian 09 by using the ωB97XD functional with the 6-311G(d,p) basis set in combination with a PCM using water as solvent to provide the lowest-energy geometries (Figure 3 and Figures S3 and S4 in

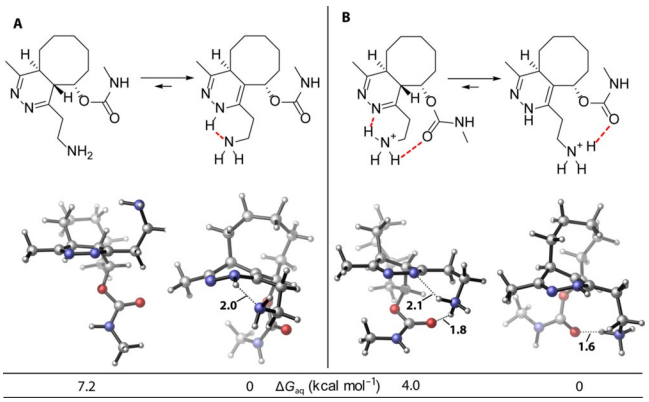

Figure 3. ωB97XD/6-311G(d)-optimized lowest-energy geometries of the dihydropyridazine adducts. Proton transfer is geometrically feasible (red lines). A) "Neutral" initial 4,5-tautomer (left) and thermodynamically favorable 1,4-tautomer (right). B) "Cationic" initial 4,5-tautomer (left) and thermodynamically favorable 1,4-tautomer (right).

the Supporting Information). The calculations show that tautomerization from the initial 4,5-dihydropyridazine towards the eliminating 1,4-dihydropyridazine appears energetically favorable and also show a prominent interaction between the aminoethyl functionality and the N-1 atom of the dihydropyridazine core in both the neutral (1,4-tautomer) (Figure 3 A) and cationic (4,5-tautomer) state (Figure 3 B). The hypothetical proton transfer through a six-membered-cyclic transition state is geometrically feasible in the kinetically favored "head-to-head" adduct and likely to facilitate both tautomerization and elimination (Scheme 1). The design consideration described above, supported by the calculations, indicates that the tetrazines **4**–**7** would show fast and pH-independent kinetics for the "click-to-release" reaction.

Synthesis

To test this hypothesis, we synthesized a library of amino-functionalized tetrazines (**4**–**17**, Scheme 2). Readily accessible *N*-Boc-protected amino-nitriles **18**–**20** were prepared in good (**20**) to quantitative yields (**18**, **19**) by treatment of the corresponding aminoalkylated precursors with di-*tert*-butyl dicarbonate in the presence of an appropriate base. Compounds **18**–**20** were subsequently converted into the *N*-Boc-protected aminoalkyltetrazines **4b**–**17b** according to the well-established method involving Lewis acid catalyzed condensation of nitriles with hydrazine followed by oxidation with sodium nitrite under acidic conditions.[17] Optimization of this two-step synthetic protocol was required to ensure the successful synthesis of each tetrazine (Table 1). At the condensation stage, five variables were altered (co-solvent, catalyst, reaction container, temperature, and reaction time) to obtain the required individually tailored conditions for each tetrazine. Altering one of these variables generally led to poor or no product formation at all. Dioxane was required as a co-solvent for the synthesis of **4b**, **5b**, **8b**, **13b**, and **17b** to ensure efficient formation of the dihydrotetrazine intermediate. The catalysts used were limited to $Zn(OTf)_2$, $Ni(OTf)_2$, and ZnI_2 due to their successful use in literature.[17a] Overall $Zn(OTf)_2$ was the preferred catalyst; however, $Ni(OTf)_2$ worked well in the reactions with MeCN as the nitrile component (**5b**, **13b**). The condensation step in the reactions towards compounds **6b**, **9b**–**11b**, **14b**, and **15b** was performed in a round-bottomed flask under an inert atmosphere ("Flask"), whereas the other reactions were executed in closed pressure-resistant test-tubes ("Tube"). A closed setup prevents the loss of ammonia, which was formed as a side-product in the condensation stage and apparently has a beneficial effect on the solubility of the components present during this stage. However, we did not observe a consistent improvement in the yields for all tetrazines when executing the condensation stage in a closed vessel. The reaction temperature and time were adjusted simultaneously. Thus, the condensa-

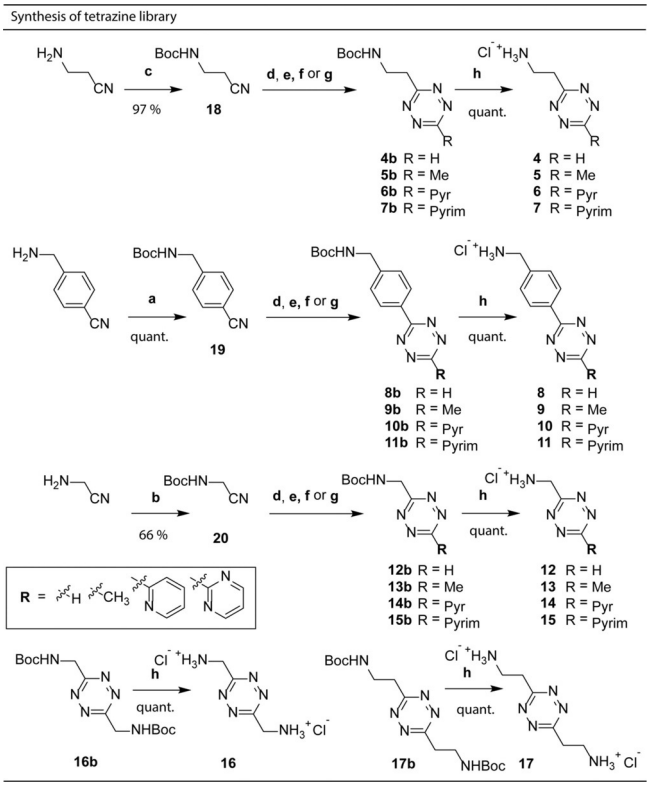

Scheme 2. Synthesis of the tetrazine library **4b**–**17b** and **4**–**17** from amino-nitriles **18**–**20**. Reagents and conditions: (a) Boc_2O, NaOH, H_2O; (b) Boc_2O, TEA, DCM; (c) Boc_2O, DCM; (d) NH_2NH_2, $Zn(OTf)_2$, formamidine acetate, then $NaNO_2$ oxidation; (e) NH_2NH_2, $Ni(OTf)_2$, acetonitrile, then $NaNO_2$ oxidation; (f) NH_2NH_2, $Zn(OTf)_2$, 2-cyanopyridine, then $NaNO_2$ oxidation; (g) NH_2NH_2, $Zn(OTf)_2$, 2-cyanopyrimidine, then $NaNO_2$ oxidation; (h) 4 M HCl, dioxane/DCM (1:1, v/v).

Table 1. Effects of varying the experimental parameters on the synthesis of *N*-Boc-protected tetrazines **4b**–**17b** en route to tetrazines **4**–**17**.

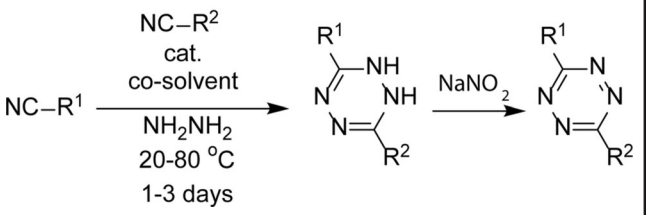

R^1	R^2	Co-solvent	Cat.	Container	T [°C]	t[a]	Yield [%]	Tetrazine
19	formamidine acetate	dioxane	$Zn(OTf)_2$	tube	60	o.n.	34	**8b**
20		–	ZnI_2	tube	30	3 d	14	**12b**
18		dioxane	$Zn(OTf)_2$	tube	20	3 d	6	**4b**
19	MeCN	–	$Zn(OTf)_2$	flask	80	o.n.	31	**9b**
20		dioxane	$Ni(OTf)_2$	tube	60	o.n.	23	**13b**
18		dioxane	$Ni(OTf)_2$	tube	60	o.n.	16	**5b**
19	PyrCN	–	$Zn(OTf)_2$	flask	80	o.n.	53	**10b**
20		–	$Zn(OTf)_2$	flask	60	o.n.	49	**14b**
18		–	$Zn(OTf)_2$	flask	60	o.n.	13	**6b**
19	PyrimCN	–	$Zn(OTf)_2$	flask	80	o.n.	7	**11b**
20		–	$Zn(OTf)_2$	flask	60	o.n.	16	**15b**
18		–	$Zn(OTf)_2$	tube	60	o.n.	27	**7b**
20	formamidine acetate	–	ZnI_2	tube	30	3 d	18	**16b**
18	PyrCN	dioxane	$Zn(OTf)_2$	tube	60	o.n.	20	**17b**

[a] o.n. = overnight.

tion reactions that required lower temperatures (20–30 °C) were left to react for 3 days, whereas those at higher temperatures (60–80 °C) were left to react overnight.[17]

The oxidation of the formed dihydrotetrazine intermediates was facilitated by transferring the reaction mixture to a 1:1 solution of AcOH and DCM followed by the addition of solid $NaNO_2$.[17b] For the oxidation of the dihydrotetrazine intermediates of tetrazines **4b**, **6b**, and **13b**, a solution of $NaNO_2$ in aqueous HCl was used, a standard reagent described in the literature to oxidize dihydrotetrazines of different nature.[17a] *N*-Boc-protected symmetric bis(aminoalkyl)tetrazines **16b** and **17b** were formed as side-products in the synthesis of tetrazines **12b** and **6b**, respectively.

The *N*-Boc protective group could be readily removed under anhydrous acidic conditions (4 M HCl in dioxane) without decomposition of the tetrazine core to yield the target aminoalkyltetrazines **4**–**17** in quantitative yields.

Determination of elimination kinetics

With the library of tetrazines (**4**–**17**) in hand, we determined their elimination behavior and compared them with those of the tetrazines reported in the literature, either "releasing" (**1**, **2**, **25**) or "nonreleasing" (**23**, **24**; Figure 4A). To probe the importance of the intramolecular proton delivery by the aminoethyl functionality we included *N*-Boc-protected tetrazines **4b**–**17b** and tetrazines **8**–**16** in which the amino group was expected to be unable to provide intramolecular assistance due to its suboptimal position.

To assess the elimination properties of all the tetrazines a direct fluorescence-based assay[13a] was chosen to monitor the reaction mixtures in real time during the elimination process. This method was preferred over a LC-MS-based analysis[13a,b] as it allows rapid measurement of several tetrazines simultaneously, acquisition of more data (at the initial stage of the reaction), and is not affected by possible "pseudo-release" artefacts caused by LC-MS analysis.[13b]

The tetrazine elimination properties were assessed by reaction with fluorogenic 2-TCO-protected 7-amino-4-methylcoumarin (2-TCO-AMC, **28**)[13a] and tracking the product AMC (**27**) by measuring its characteristic fluorescence at 450 nm (Figure 4B and Figures S5 and S6 in the Supporting Information). Initially we tested the literature tetrazines in both DMSO/H_2O (1:1, v/v) and phosphate-buffered saline (PBS; 0.25% DMSO, Figure 4C, right panel, and Figure S8). The elimination properties in PBS were vastly different compared with in DMSO/H_2O. With tetrazine **2**, for example, the elimination was both faster and more efficient in PBS (Figure 4C, left panel). As a result, we focused on the experiments conducted in PBS. The elimination efficiencies (Eff%) and rate constants (k_{elim}) of the tetrazine library were determined by exposing 2-TCO-AMC (5 μM) to four equivalents (20 μM) of tetrazine in PBS (pH 7.4) at 37 °C for 8 days (see Figures S7–S13). At various times, the fluorescence intensity relative to 2-TCO-AMC (0%) and AMC (100%) was quantified (see Figures S14 and S15). The solvent and concentrations were chosen to be relevant to experiments conducted in biological systems.

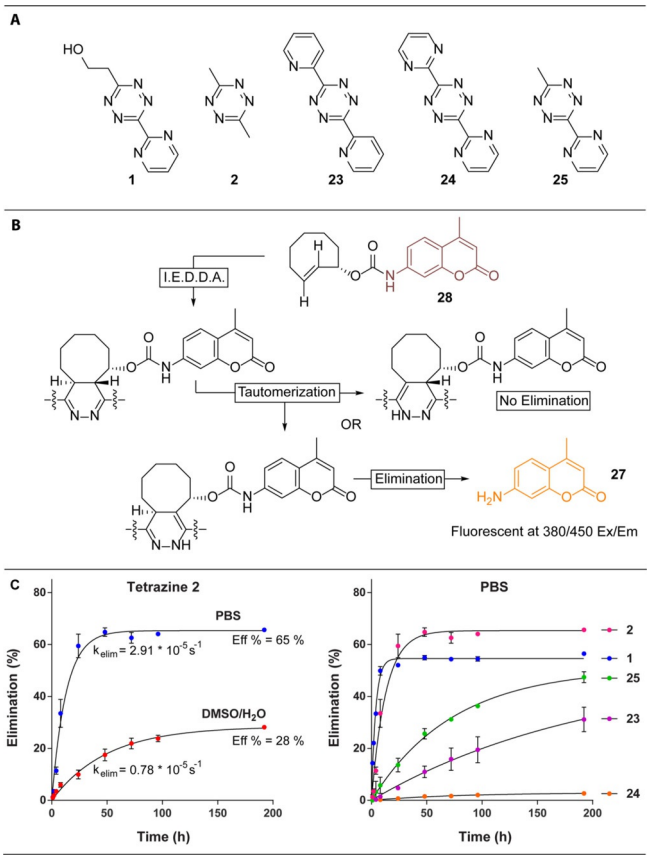

Figure 4. A) Tetrazines **1**, **2**, and **23**–**25** used as literature references. B) Fluorescence-based assay: Fluorogenic 2-TCO-AMC (**28**) was used as a measurement tool to track the release of fluorescent AMC (**27**) upon reaction with tetrazines. C) Data obtained in DMSO/H_2O (**2**, left panel) or PBS (**1**, **2**, **23**–**25**, right panel) as solvent during the fluorescence-based assay.

The data obtained were analyzed and the rate constant (k_{elim}) and efficiency (Eff%) were determined for each tetrazine. The values for all the tetrazines were plotted as dots in an *XY* scatter plot as k_{elim} (logarithmic scale) versus Eff% (linear scale; Figure 5A). Three classes of tetrazines are most conspicuous: Tetrazines **14b**, **15b**, **23**, and **11** showed low elimination rate constants ($k_{elim} < 0.20 \times 10^{-5}$ s^{-1}; Figure 5B), tetrazines **11b**, **2**, **5**, and **17** all displayed intermediate elimination rate constants ($k_{elim} = (1.5–3.0) \times 10^{-5}$ s^{-1}; Figure 5C), and tetrazines **1**, **4**, **6**, and **7** form a third, most interesting, class of tetrazines defined by their very fast release kinetics (Figure 5D). Although the reaction with reference tetrazine **1** is fast ($k_{elim} = 8.86 \times 10^{-5}$ s^{-1}), it is still significantly slower than those with **4**, **6**, and **7** ($k_{elim} = 15.3 \times 10^{-5}$, 23.7×10^{-5}, and 35.9×10^{-5} s^{-1}, respectively). The release rates for tetrazines **4**, **6**, and **7** were too high to be accurately determined by our initial assay and therefore the minimum rate constants to be recorded have been given. It is noteworthy that the tetrazines with a protected amino group (**14b**, **15b**) and the tetrazine with a suboptimal-positioned amino group (**11**) show low elimination rate constants (Figure 5B). This behavior proved to be general across the whole test set (see Figures S7–S13 in the Supporting Information) and underscores the importance of the intramolecular proton delivery for the rate of the "click-to-release" process.

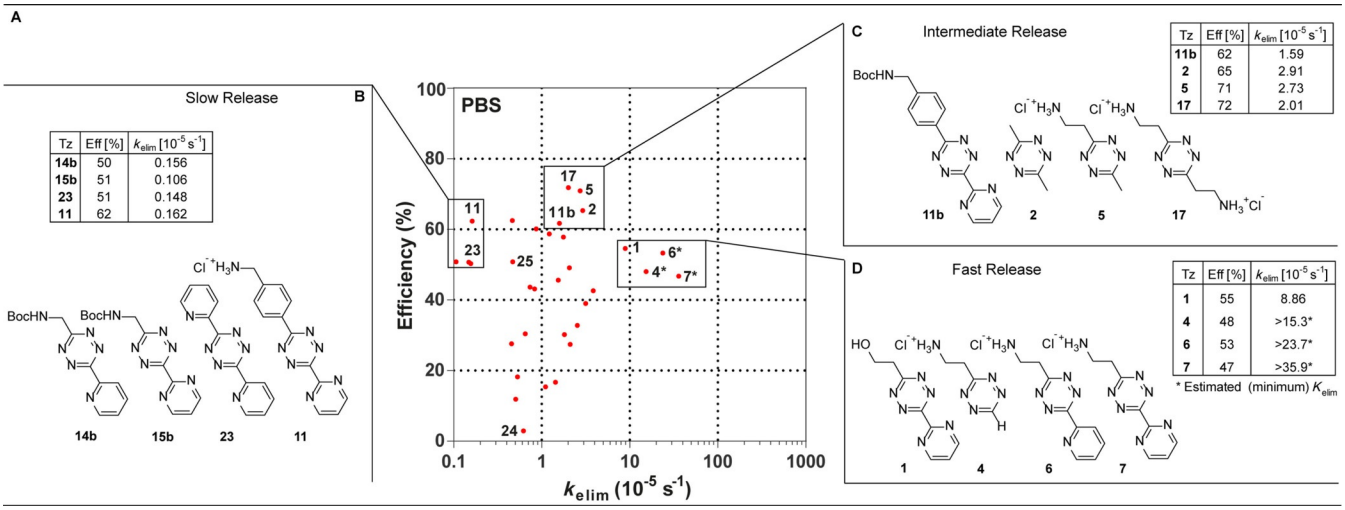

Figure 5. A) *XY* scatter plot of all the data obtained in PBS as solvent during the fluorescence-based assay. Each result (tetrazines **1**, **2**, **23**–**25**, **4b**–**17b**, **4**–**17**) is depicted as a dot based on their elimination efficiency and rate constant. B) Tetrazines **14b**, **15b**, **23**, and **11** with slow release properties ($k_{elim} < 0.2 \times 10^{-5}$ s^{-1}). C) Tetrazines **11b**, **2**, **5**, and **17** with intermediate release properties (Eff% > 60%). D) Tetrazines **1**, **4**, **6**, and **7** with fast release properties ($k_{elim} > 8 \times 10^{-5}$ s^{-1}).

pH dependency of elimination rates

Following these results we set out to determine whether the fast-releasing aminoethyl-functionalized tetrazines retained these properties over a wide pH range. To this end, tetrazines **1**–**3**, **21**, **4b**–**7b**, and **4**–**7** were exposed to phosphate-buffered solutions at various pH (0.2 M PO_4^{2-}, 10% DMSO, pH 3.0, 6.0, and 7.4). At pH 3.0 (Figure 6A and Figures S16–S18 in the Supporting Information), all the tetrazines show elimination rate constants between 30×10^{-5} and 500×10^{-5} s^{-1}, which indicates that the availability of protons in solution enhances the elimination rate. Lowering the proton concentration by raising the pH to 6.0 or 7.4 resulted in large decreases in the elimination rates for most tetrazines (Figure 6B,C and Figures S16–S18). At pH 7.4, tetrazines **1**–**3**, **21**, **6b**, and **7b** show much lower elimination rate constants ($k_{elim} = (5–15) \times 10^{-5}$ s^{-1}, Figure 6C). Aminoethyltetrazines **6** ($k_{elim} = 241 \times 10^{-5}$ s^{-1}) and **7** ($k_{elim} = 120 \times 10^{-5}$ s^{-1}), on the other hand, showed a minimal reduction in rate at increased solvent pH (Figure 7), with rates 18–27-fold higher than those given above at pH 7.4. Substituting amino (**6**, **7**) for an alcohol (**1**) or carbamate (**6b**, **7b**) functionality reintroduced pH dependency into the elimination process (Figure 8). A carboxy functionality, as seen in tetrazine **3**, provided an overall moderate elimination rate and moderate pH

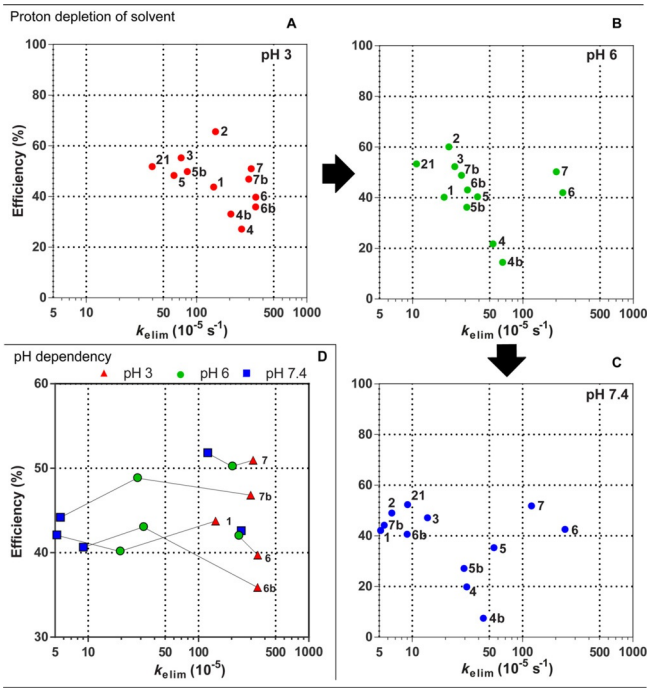

Figure 6. Proton depletion of solvent. A) Scatter plot of tetrazines at pH 3. B) Scatter plot of tetrazines at pH 6. C) Scatter plot of tetrazines at pH 7.4. D) Scatter plot of pH-dependent tetrazines **6** and **7** and pH-independent tetrazines **6b**, **7b**, and **1**.

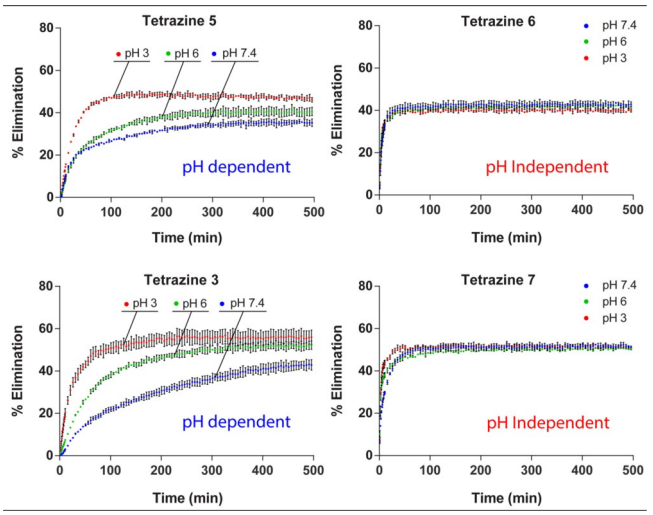

Figure 7. Time-dependent elimination of tetrazines **3** and **5**–**7** showing pH-dependent and pH-independent behavior.

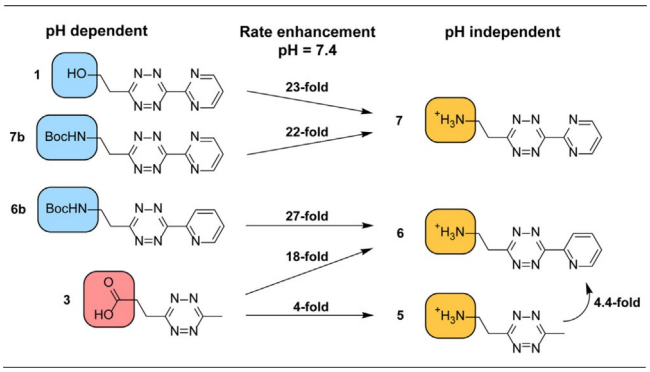

Figure 8. Rate enhancement of pH-independent functional groups depicted in orange over pH-dependent functional groups depicted in blue and red.

dependency (Figure 8). Substitution of the carboxy (**3**) for an amino (**5**) functionality improved both properties. Furthermore, the most reactive tetrazine **6** outperforms tetrazine **3** by 18-fold in terms of elimination rate. Finally, when comparing tetrazines **4**–**7**, the data also show that the elimination rate is positively affected by electron-withdrawing substituents (pyridine, pyrimidine), which explains the differences between the tetrazines, in line with previous findings.[13b]

These results strongly support our hypothesis that the elimination process is dependent on proton availability and can be catalyzed at biologically relevant pH (3–7.4) through careful placement of the cationic ammonium functionality acting as an intramolecular catalyst.

LC-MS analysis

To gain additional insight into the course of the "click-to-release" reaction with the newly developed aminoalkyltetrazines and to study the intermediates and possible side-products, we also assessed the elimination rates of the key compounds **5**–**7** by means of the reported LC-MS-based approach that uses an ammonium formate buffered water/acetonitrile solution as eluent (2.5 mM $NH_4^+HCOO^-$, pH 8.4), taking the first analysis point at $t = 5$ min.[13b] The known tetrazines **1**–**3** were analyzed by this method for comparison. The elimination rates with tetrazines **2** and **3** corresponded to the data reported by Weissleder and co-workers,[13b] with tetrazine **3** giving 48% release at $t = 5$ min rising to 72% after 16 hours (Figure 9). The explanation offered by the authors invokes a rapidly releasing "head-to-head" adduct and a slowly releasing "head-to-tail" adduct that are formed in approximately equal amounts.[13b] The data show much faster initial release than measured in the fluorescence assay, and this is likely due to additional "pseudo-release" or concentration effects during the LC-MS analysis. In turn, aminoethyltetrazines **5**, **6**, and **7** showed 78, 80, and 70% initial release, respectively, at $t = 5$ min with only a small further increase in release over time (Figure 9). This would correspond to the preferential formation of the rapidly releasing "head-to-head" adduct as predicted by our calculations.

It is noteworthy that although we observed a multitude of different intermediates, including putative "head-to-tail" and

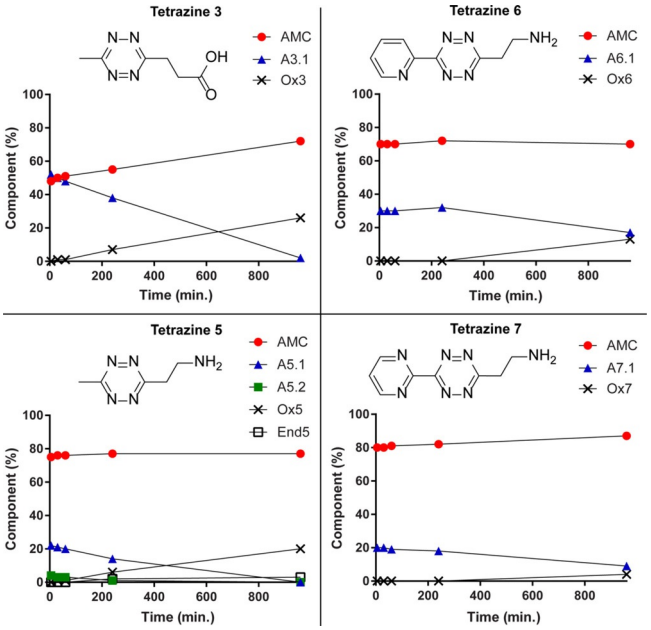

Figure 9. Time-dependent LC-MS analysis of the reaction of 2-TCO-AMC (**28**) with tetrazines **3** and **5**–**7** in PBS.

"head-to-head" adducts, in the reaction of 2-TCO-AMC (**28**) with the comparatively slow eliminating tetrazines **1** and **2** (Figure 10 and Figures S19 and S20 in the Supporting Information) as well as with tetrazines **3** and **5**–**7** (Figure 9 and Figures S21–S24), we did not consistently see the formation of a dead-end adduct (End) as reported by others.[13b] Furthermore, the amount of the oxidized adduct (Ox) is reduced for tetrazines **1**, **6**, and **7** compared with for tetrazines **2**, **3**, and **5**. The results of the LC-MS analysis of the "click-to-release" reaction

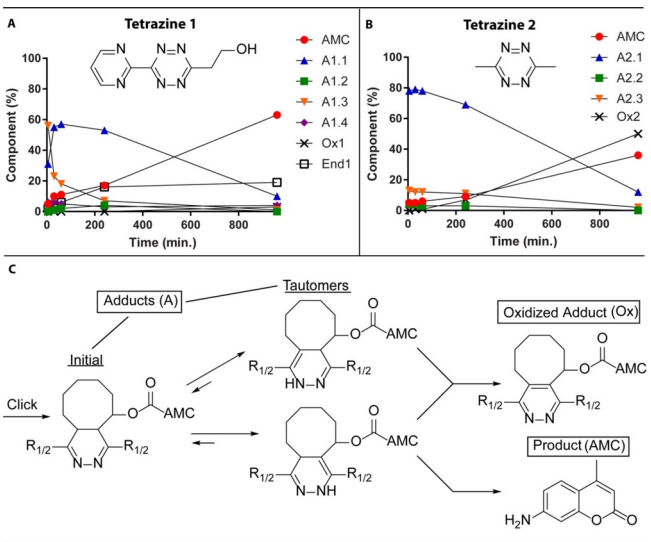

Figure 10. Time-dependent LC-MS analysis of the reaction of 2-TCO-AMC (**28**) with tetrazines in PBS. A) Reaction of **28** with tetrazine **1**. B) Reaction of **28** with tetrazine **2**. C) Elimination pathway showing the possible adducts and products. Aminomethylcoumarin-containing molecules: product "AMC", adducts "A", oxidized adduct "Ox", and unidentified dead-end adduct "End".

of 2-TCO-AMC (**28**) with tetrazines **1** and **2** are similar to those published by Robillard and co-workers in terms of observed intermediates and side-products (Figure 9 A,B).[13c] To summarize, the results obtained from the LC-MS analysis of the key tetrazine derivatives demonstrate that the method shows reproducible results for the known tetrazines **2** and **3** and that the aminoethyltetrazines **5**–**7** perform as designed in the "click-to-release" IEDDA reaction.

Conclusion

The full kinetic profiling of a focused tetrazine library clearly shows that the presence of a properly placed cationic ammonium functionality acting as an intramolecular proton donor gives the tetrazine-mediated "click-to-release" elimination a pH-independent character. Asymmetric tetrazines that contain both this aminoethyl substituent and an electron-withdrawing substituent on the tetrazine core show unprecedented release rates combined with nearly complete pH independence over the whole biologically relevant pH range.

Acknowledgements

A.J.C.S., D.V.F., and S.I.V.K. were funded by the Institute of Chemical Immunology (NWO Zwaartekracht), M.A.R.D.G. and S.I.V.K. were funded by the European Research Council (ERC-2014-StG-639005), and W.D. was funded by an NWO BBoL-grant. The authors thank the SURFsara for support in using the Dutch national supercomputer, including the Lisa system.

Conflict of interest

The authors declare no conflict of interest.

Keywords: bioorthogonal chemistry · Diels–Alder reactions · elimination · nitrogen heterocycles · pH effects

[1] a) D. M. Patterson, L. A. Nazarova, J. A. Prescher, *ACS Chem. Biol.* **2014**, *9*, 592; b) X. Fan, J. Li, P. R. Chen, *Natl. Sci. Rev.* **2017**, *4*, 300.

[2] a) V. V. Rostovtsev, L. G. Green, V. V. Fokin, K. B. Sharpless, *Angew. Chem. Int. Ed.* **2002**, *41*, 2596; *Angew. Chem.* **2002**, *114*, 2708; b) J. E. Hein, V. V. Fokin, *Chem. Soc. Rev.* **2010**, *39*, 1302.

[3] C. I. Schilling, N. Jung, M. Biskup, U. Schepers, S. Bräse, *Chem. Soc. Rev.* **2011**, *40*, 4840.

[4] a) M. L. Blackman, M. Royzen, J. M. Fox, *J. Am. Chem. Soc.* **2008**, *130*, 13518; b) S. Mayer, K. Lang, *Synthesis* **2017**, *49*, 830.

[5] a) E. M. Sletten, C. R. Bertozzi, *Acc. Chem. Res.* **2011**, *44*, 666; b) K. Lang, J. W. Chin, *ACS Chem. Biol.* **2014**, *9*, 16.

[6] J. Li, P. R. Chen, *Nat. Chem. Biol.* **2016**, *12*, 129.

[7] R. M. Versteegen, R. Rossin, W. ten Hoeve, H. M. Janssen, M. S. Robillard, *Angew. Chem. Int. Ed.* **2013**, *52*, 14112; *Angew. Chem.* **2013**, *125*, 14362.

[8] L. Liu, Y. Liu, G. Zhang, Y. Ge, X. Fan, F. Lin, J. Wang, H. Zheng, X. Xie, X. Zeng, P. R. Chen, *Biochemistry* **2018**, *57*, 446.

[9] G. Zhang, J. Lie, R. Xie, X. Fan, Y. Liu, S. Zheng, Y. Ge, P. R. Chen, *ACS Cent. Sci.* **2016**, *2*, 325.

[10] a) R. Rossin, S. M. J. van Duijnhoven, W. ten Hoeve, H. M. Janssen, L. H. J. Kleijn, F. J. M. Hoeben, R. M. Versteegen, M. S. Robillard, *Bioconjugate Chem.* **2016**, *27*, 1697; b) I. Khan, L. M. Seebald, N. M. Robertson, M. V. Yigit, M. Royzen, *Chem. Sci.* **2017**, *8*, 5705; c) R. Rossin, R. M. Versteegen, J. Wu, A. Khasanov, H. J. Wessels, E. J. Steenbergen, W. ten Hoeve, H. M. Janssen, A. H. A. M. van Onzen, P. J. Hudson, M. S. Robillard, *Nat. Commun.* **2018**, *9*, 1484.

[11] A. M. F. van der Gracht, M. A. R. de Geus, M. G. M. Camps, T. J. Ruckwardt, A. J. C. Sarris, J. Bremmers, E. Maurits, J. B. Pawlak, M. M. Posthoorn, K. M. Bonger, D. V. Filippov, H. S. Overkleeft, M. S. Robillard, F. Ossendorp, S. I. van Kasteren, *ACS Chem. Biol.* **2018**, *13*, 1569.

[12] J. M. M. Oneto, I. Khan, L. Seebald, M. Royzen, *ACS Cent. Sci.* **2016**, *2*, 476.

[13] a) X. Fan, Y. Ge, F. Lin, Y. Yang, G. Zhang, W. S. C. Ngai, Z. Lin, S. Zheng, J. Wang, J. Zhao, J. Lie, P. R. Chen, *Angew. Chem. Int. Ed.* **2016**, *55*, 14046; *Angew. Chem.* **2016**, *128*, 14252; b) J. C. T. Carlson, H. Mikula, R. Weissleder, *J. Am. Chem. Soc.* **2018**, *140*, 3603; c) R. M. Versteegen, W. ten Hoeve, R. Rossin, M. A. R. de Geus, H. M. Janssen, M. S. Robillard, *Angew. Chem. Int. Ed.* **2018**, *57*, 10494; *Angew. Chem.* **2018**, *130*, 10654.

[14] a) M. T. Taylor, M. L. Blackman, O. Dmitrenko, J. M. Fox, *J. Am. Chem. Soc.* **2011**, *133*, 9646; b) F. Liu, Y. Liang, K. N. Houk, *J. Am. Chem. Soc.* **2014**, *136*, 11483.

[15] Gaussian 09, M. J. Frisch, G. W. Trucks, H. B. Schlegel, G. E. Scuseria, M. A. Robb, J. R. Cheeseman, G. Scalmani, V. Barone, G. A. Petersson, H. Nakatsuji, X. Li, M. Caricato, A. Marenich, J. Bloino, B. G. Janesko, R. Gomperts, B. Mennucci, H. P. Hratchian, J. V. Ortiz, A. F. Izmaylov, J. L. Sonnenberg, D. Williams-Young, F. Ding, F. Lipparini, F. Egidi, J. Goings, B. Peng, A. Petrone, T. Henderson, D. Ranasinghe, V. G. Zakrzewski, J. Gao, N. Rega, G. Zheng, W. Liang, M. Hada, M. Ehara, K. Toyota, R. Fukuda, J. Hasegawa, M. Ishida, T. Nakajima, Y. Honda, O. Kitao, H. Nakai, T. Vreven, K. Throssell, J. A. Montgomery, Jr., J. E. Peralta, F. Ogliaro, M. Bearpark, J. J. Heyd, E. Brothers, K. N. Kudin, V. N. Staroverov, T. Keith, R. Kobayashi, J. Normand, K. Raghavachari, A. Rendell, J. C. Burant, S. S. Iyengar, J. Tomasi, M. Cossi, J. M. Millam, M. Klene, C. Adamo, R. Cammi, J. W. Ochterski, R. L. Martin, K. Morokuma, O. Farkas, J. B. Foresman, D. J. Fox, Gaussian, Inc., Wallingford CT, **2016**.

[16] Spartan'10, Wavefunction, Inc. Irvine, CA.

[17] a) J. Yang, M. R. Karver, W. Li, S. Sahu, N. K. Devaraj, *Angew. Chem. Int. Ed.* **2012**, *51*, 5222; *Angew. Chem.* **2012**, *124*, 5312; b) K. Lang, L. Davis, S. Wallace, M. Mahesh, D. J. Cox, M. L. Blackman, J. M. Fox, J. W. Chin, *J. Am. Chem. Soc.* **2012**, *134*, 10317.

Manuscript received: July 27, 2018

Accepted manuscript online: September 5, 2018

Version of record online: November 8, 2018